Stability analysis of laminate plates by the boundary element method

S. Syngellakis & N. Cherukunnath
School of Engineering Sciences, University of Southampton, U.K.

Abstract

A numerical analysis of laminate plate buckling, based on the boundary element method (BEM), is presented. Bending-stretching coupling is ignored and uniform in-plane edge loading is assumed. Integral equations containing an irreducible domain integral depending on the plate deflection are derived from a reciprocity relation using the fundamental solutions of the anisotropic plate bending problem. Boundary modelling is combined with deflection modelling over the plate so that three integral equations are approximated as a discrete system of equations forming an eigenvalue problem from which the critical load can be evaluated. This approach removes the need for integral equations involving the domain curvatures yielding directly the buckling mode of the plate. Linear discontinuous boundary elements as well as domain cells are employed combined with special schemes for the approximation of jump terms at corners. Singular integrals over elements containing the source point are evaluated from closed-form expressions derived through analytical integration. The C code implementing the solution algorithm is applied to several benchmark problems involving orthotropic plates and BEM predictions are compared with solutions available from the literature or obtainable through a general purpose finite element package. The reliability of the proposed analysis is established through further applications to laminate plates of general anisotropy.

1 Introduction

Laminates can be engineered to meet the specific demands of a particular application but the complexities in their mechanical behaviour demanded the development of new methods for their analysis. A detailed and accurate calculation of laminate stresses and deformation is required for design purposes.

Buckling is a type of behaviour that may cause catastrophic component failure. Closed form solutions for the critical load of laminates modelled as anisotropic elastic plates have been found in a few simple cases involving regular shapes as well as uniform loading and support conditions [1]. In more general cases, the problem has been solved using various numerical techniques. The objective of this paper is to present one computer implemented boundary element solution of the general problem and to demonstrate its accuracy through the solution of a number of benchmark problems covering a range of common loading and support conditions.

The plate buckling problem does not possess a closed form fundamental solution valid for any membrane stress distribution. Thus a genuine boundary integral equation that can be approximated by established boundary element methodology is not available. For this reason, integral equations have been derived using the fundamental solutions of plate bending problem. Such BEM formulations for isotropic plates included irreducible domain integrals depending on the curvatures [2], which were modelled as additional nodal unknowns in a discretized domain. This approach has been extended to the stability analysis of orthotropic plates [3, 4]. In all these applications, constant boundary elements were used and results were obtained for uniformly loaded, simply-supported or clamped rectangular plates.

The analysis presented in this paper is based on a transformation of the integral equation of the problem so that the deflection replaces the curvatures in the irreducible domain integral. Thus only one additional integral equation is required for the generation of a consistent equivalent system of approximate algebraic equations. The deflection is the only domain unknown which needs to be modelled over two-dimensional cells. The present work constitutes an extension to earlier boundary element solutions for isotropic plates [5, 6]. Linear discontinuous interpolation models over boundary elements and domain cells are used. Uniform pre-buckling membrane states and simple combinations of edge conditions have been assumed. The critical load factor is determined from a standard eigenvalue problem. The developed C codes are verified through extensive application to a series of bench mark problems and comparison of their predictions with exact or other numerical results.

2 Constitutive equations

Laminates are usually produced by stacking thin unidirectionally reinforced layers at different fibre orientations. The effective properties of a laminate vary with the reinforcement orientation, thickness, and stacking sequence of the individual layers. The simplest lamination theory is based on the assumptions that the layers are perfectly bonded, the material of each layer is homogeneous with known effective properties and each layer is in a state of plane stress. The laminate is also expected to deform according to Kirchhoff's assumptions for the bending of thin plates.

According to the above theory applied to mid-plane symmetrically laminated plates, in which bending-stretching coupling does not arise, the bending moments $M_{\alpha\beta}$ are related to the curvatures $\kappa_{\alpha\beta}$ by

$$M_{\alpha\beta} = D_{\alpha\beta\gamma\delta}\kappa_{\gamma\delta} \tag{1}$$

where $D_{\alpha\beta\gamma\delta}$ are the flexural stiffness coefficients or flexural rigidities and the range of Greek indices is (1, 2). Tensor notation relative to a Cartesian frame of reference x_1, x_2, and the summation convention over repeated indices have been used. The curvatures $\kappa_{\alpha\beta}$ are given in terms of the deflection w by

$$\kappa_{\alpha\beta} = -w_{,\alpha\beta} \tag{2}$$

where a comma followed by a lower index indicates differentiation with respect to the corresponding co-ordinate.

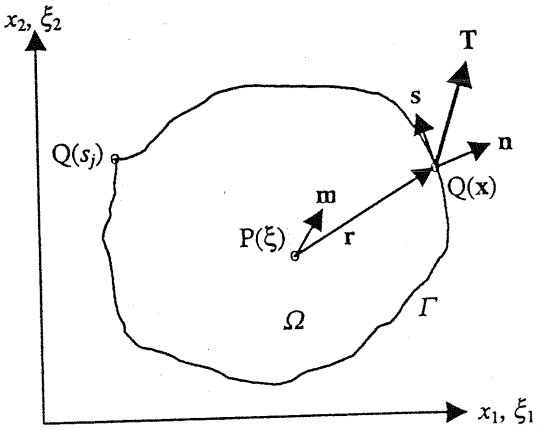

Figure 1: Plate geometry notation

3 Critical equilibrium

The plate is assumed loaded by only a factored edge load λT_α, which generates a membrane state of stress $\lambda N_{\alpha\beta}$. This equilibrium state becomes unstable at a certain critical value of the factor λ. Then a second stable equilibrium state exists, associated with the so called buckling mode $w(x_\alpha)$.The critical load factor λ_c and the buckling mode can be determined from a variational equation [7]

$$\Pi(w,\delta w) = \int_\Omega D_{\alpha\beta\gamma\delta}\, w_{,\alpha\beta}\, \delta w_{,\gamma\delta}\, d\Omega + \lambda_c \int_\Omega N_{\alpha\beta}\, w_{,\alpha}\, \delta w_{,\beta}\, d\Omega = 0 \tag{3}$$

where δ is the variational symbol, $N_{\alpha\beta}$ are the membrane forces, Ω is the plate domain bounded by the contour Γ, which is smooth apart from a finite number K of corner points as shown in Fig. 1.

Repeated integration by parts and application of Green's theorem transforms eqn (3) to:

$$\int_{\Omega}(D_{\alpha\beta\gamma\delta}\,w_{,\alpha\beta\gamma\delta}-\lambda_c N_{\alpha\beta}\,w_{,\alpha\beta}\,)\delta w\mathrm{d}\Omega$$

$$+\int_{\Gamma}[(V_n+\lambda_c T_\alpha w_{,\alpha}\,)\delta w-M_n\delta\theta_n]\mathrm{d}\Gamma+\sum_{j=1}^{K}C_j\delta w_j=0 \tag{4}$$

where the normal slope θ_n, shear force V_n and bending moment M_n along the boundary are given by

$$\theta_n=\frac{\partial w}{\partial n}$$

$$V(w)=-D_{\alpha\beta\gamma\delta}\left[n_\delta\,w_{,\alpha\beta\gamma}+\frac{\partial}{\partial s}(n_\gamma s_\delta\,w_{,\alpha\beta}\,)\right] \tag{5}$$

$$M_n(w)=-D_{\alpha\beta\gamma\delta}n_\gamma n_\delta w_{,\alpha\beta} \tag{6}$$

and the forces C_j are equal to discontinuity jumps of the twisting moment

$$M_{ns}(w)=-D_{\alpha\beta\gamma\delta}n_\gamma s_\delta w_{,\alpha\beta} \tag{7}$$

at the corners.

The condition that eqn (4) be satisfied for an arbitrary δw yields the field equation

$$D_{\alpha\beta\gamma\delta}\,w_{,\alpha\beta\gamma\delta}-\lambda_c N_{\alpha\beta}w_{,\alpha\beta}=0 \tag{8}$$

over the domain Ω and the boundary conditions,

$$\text{either } M_n=0 \text{ or } \theta_n=\overline{\theta}\,(s) \tag{9}$$

$$\text{either } V+\lambda_c T_\alpha w_{,\alpha}=0 \text{ or } w=\overline{w}\,(s) \tag{10}$$

on Γ and

$$\text{either } C(s_j)=0 \text{ or } w_j=\overline{w}\,(s_j);\ j=1,\ldots,K \tag{11}$$

at the corners, where $\overline{\theta}\,(s)$ and $\overline{w}\,(s)$ are, respectively, prescribed values of the slope and deflection along the whole or part of the boundary. The boundary element method will be applied to the numerical solution of the boundary value problem described by eqn (8) and conditions (9)-(11).

4 Integral equations

The present formulation is based on the integral equation (4) in which δw is replaced by a weighting function w^*. A second such integral equation results from interchanging the roles of w and w^* in eqn (4). The difference of the left-hand sides of these two integral equations is

$$\int_{\Omega}D_{\alpha\beta\gamma\delta}\,(w_{,\alpha\beta\gamma\delta}\,w^*-w^*{}_{,\alpha\beta\gamma\delta}\,w)\mathrm{d}\Omega-\lambda_c[I^d(w,\ w^*)-I^d(w^*,w)]$$

$$+I^b(w,\ w^*)+\lambda_c I^r(w,\ w^*)+J(w,\ w^*)=0 \tag{12}$$

where

$$I^d(w,\ w^*)=\int_{\Omega}N_{\alpha\beta}\,w_{,\alpha\beta}\ w^*\delta\Omega \tag{13}$$

$$I^b(w,\ w^*) = \int_\Gamma \left[V(w)w^* - M_n(w)\theta_n^* + M_n(w^*)\theta_n - V(w^*)w\right]\mathrm{d}\Gamma \qquad (14)$$

$$I^t(w,\ w^*) = \int_\Gamma T_\alpha(w_{,\alpha}\ w^* - w^*_{,\alpha}\ w)\mathrm{d}\Gamma \qquad (15)$$

$$J(w,\ w^*) = \sum_{j=1}^{K} [C_j(w)w^*(s_j) - C_j(w^*)w(s_j)] \qquad (16)$$

Two terms in the domain integrals of eqn (12) are eliminated by identifying $w(x_\alpha)$ with the buckling mode and taking into account eqn (8). Since an explicit fundamental solution of eqn (8), valid for any membrane stress distribution, is not available, the present formulation adopts as weighting function w^* the fundamental solutions w_1^* and w_2^* of the plate bending problem. These are interpreted as deflections at a field point Q(**x**) of an infinite plate, w_1^* due to a lateral unit point force, w_2^* due to a unit bending moment, both acting at the source point P(ξ), with the plane of the bending moment specified through the unit vector **m** at an angle α to the position vector $\mathbf{r} = \mathbf{x} - \xi$ (Fig.1). Complete expressions for both fundamental solutions can be found in Shi and Bezine's BEM analysis of anisotropic plate bending [8].

Integral equation (12) is thus transformed to

$$-kw_i + I^b(w, w_i^*) + \lambda_c[I^t(w, w_i^*) + I^d(w_i^*, w)] + J(w, w_i^*) = 0;\ i = 1,2 \qquad (17)$$

where

$$w_1 = w(\xi),\ \ w_2 = \theta_n(\xi)$$

k is equal to either 1 or 0.5 depending on whether P(ξ) is in the domain or on a smooth portion of the boundary, respectively. Due to the presence of the domain integral $I^d(w_i^*, w)$ depending on the unknown deflection, eqn (17) is not a proper boundary integral equation. Despite this mathematical complication, the boundary element methodology can still be applied to the present problem by introducing a simple model for the domain deflection, complementing the conventional boundary modelling.

5 Boundary and domain models

The boundary integrals $I^b(w, w_i^*)$ and $I^t(w, w_i^*)$, defined by eqns (14) and (15), respectively, depend on the four variables w, θ_n, V and M_n. Accounting for the boundary conditions, only two from those are unknown quantities which need to be approximated over boundary elements. The linear discontinuous model has been adopted in the present analysis. This model not only represents more accurately the variation of a boundary variable but also allows a more direct modelling of its discontinuity at a corner. Since there are two independent unknowns per node, the total number of boundary unknowns will be N_b=4N_e where N_e is the number of boundary elements.

If Z denotes a boundary unknown, a typical boundary integral over an individual element Γ_e would have the form

$$I^e = \sum_{k=1}^{2} Z_k \int_{\Gamma_e} G\phi_k \mathrm{d}\Gamma \tag{18}$$

where G would be the kernel paired with variable Z in integral equation (17) and ϕ_k are the interpolation functions. The integration over elements which do not contain the source point are performed numerically using Gaussian quadrature. Analytical integration is however possible over elements containing the source point. This removes the need for elaborate numerical schemes to deal with the singularities of certain kernels and leads to better accuracy.

The modelling of the jump term at corners requires a relation between the twisting moment M_{ns} and some boundary unknowns or their path derivatives. Such a relation is derived by transforming the constitutive equations at the boundary relative to a local **n**-**s** frame of reference where $\mathbf{s}(s_1,s_2)$ is a unit vector tangent to the edge contour (Fig. 1). Referring to eqns (6) and (7), this transformation needs only to be applied to $w_{,\alpha\beta}$ which becomes

$$w_{,\alpha\beta} = n_\alpha n_\beta \frac{\partial^2 w}{\partial n^2} + (n_\alpha s_\beta + s_\alpha n_\beta)\frac{\partial^2 w}{\partial n \partial s} + s_\alpha s_\beta \frac{\partial^2 w}{\partial s^2} \tag{19}$$

Substituting eqn (19) into eqns (6) and (7) and eliminating $\partial^2 w/\partial n^2$ between them, results in an expression for M_{ns} in terms of M_n, $\partial\theta_n/\partial s$ and $\partial^2 w/\partial s^2$. Using the adopted boundary element model, an approximation can thus be deduced for the twisting moment appearing in the jump term over the boundary elements adjacent and on either side of a corner in terms of the nodal values of M_n, θ_n and w within these elements.

The domain integral $I^d(w_i^*,w)$ in eqn (17) is evaluated by modelling the deflection over the plate domain, which is discretized into N_c triangular domain cells. Linear interpolation functions of the form

$$\phi_i = \sum_{j=1}^{3} \alpha_{ij}\zeta_j \tag{20}$$

were adopted where ζ_j, j = 1,2,3, are the familiar area co-ordinates. The three internal nodes were placed along the medians halfway between the vertices and the cell centroid [6]. Thus the total number of internal nodes is $N_d = 3N_c$.

6 The algebraic problem

Boundary and domain models are substituted into eqn (17), the source point placed at all boundary nodes and integrations are carried out over all elements leading to the following system of N_b linear algebraic equations

$$(\mathbf{H}^b + \lambda_c \mathbf{H}^i)\,\mathbf{Z} = \lambda_c \mathbf{H}^d \mathbf{W} \tag{21}$$

where **Z** and **W** are the arrays containing the boundary and domain unknowns, respectively, the elements of matrix $\mathbf{H}^b$ result from integrals $I^b(w, w_i^*)$ and jump

terms $J(w, w_i^*)$, while matrices $\mathbf{H}^t$ and $\mathbf{H}^d$ are the consequence of integrals $I^t(w, w_i^*)$ and $I^d(w_i^*, w)$, respectively. An additional system of N_d equations,

$$(\mathbf{D}^b + \lambda_c \mathbf{D}^t)\,\mathbf{Z} = (\mathbf{I} + \lambda_c \mathbf{D}^d)\mathbf{W} \tag{22}$$

is obtained by applying equation (17) with $k = i = 1$ and placing the source point at all domain nodes. Then, integrals $I^b(w, w_1^*)$, $I^t(w, w_1^*)$ and $I^d(w_1^*, w)$ would generate the elements of matrices $\mathbf{D}^b$, $\mathbf{D}^t$ and $\mathbf{D}^d$, respectively, with the jump terms contributing to $\mathbf{D}^b$.

The critical load factor is the smallest eigenvalue of the system of equations (21) and (22) which can be written as a standard eigenvalue problem

$$(\mathbf{A} - \lambda_c \mathbf{B})\,\mathbf{X} = \mathbf{0} \tag{23}$$

where

$$\mathbf{A} = \begin{bmatrix} \mathbf{H}^b & \mathbf{0} \\ \mathbf{D}^b & -\mathbf{I} \end{bmatrix}, \mathbf{B} = \begin{bmatrix} -\mathbf{H}^t & \mathbf{H}^d \\ -\mathbf{D}^t & \mathbf{D}^d \end{bmatrix}, \mathbf{X} = \begin{Bmatrix} \mathbf{Z} \\ \mathbf{W} \end{Bmatrix}$$

Thus λ_c^{-1} can be evaluated as the largest eigenvalue of matrix $\mathbf{A}^{-1}\mathbf{B}$ which can be directly obtained from

$$\mathbf{A}^{-1}\mathbf{B} = \begin{bmatrix} -\hat{\mathbf{H}}^b \mathbf{H}^t & \hat{\mathbf{H}}^b \mathbf{H}^d \\ -\mathbf{D}^b \hat{\mathbf{H}}^b \mathbf{H}^t + \mathbf{D}^t & \mathbf{D}^b \hat{\mathbf{H}}^b \mathbf{H}^d - \mathbf{D}^d \end{bmatrix}$$

where $\hat{\mathbf{H}}^b = (\mathbf{H}^b)^{-1}$. Thus the inversion of only the $N_b \times N_b$ matrix $\mathbf{H}^b$ is required while efficient routines yielding the largest eigenvalue of a matrix as well as the associated eigenvector are readily available [9]. It is worth noting that boundary integral $I^t(w, w_i^*)$ vanishes under certain combinations of loading and support conditions. These include simply supported and clamped plates under edge shear anywhere on the boundary as well as compression on the clamped portion of the boundary. In such cases, both matrices $\mathbf{H}^t$ and $\mathbf{D}^t$ vanish and the eigenvalue problem (23) reduces further to

$$[(\mathbf{D}^b \hat{\mathbf{H}}^b \mathbf{H}^d - \mathbf{D}^d) - \lambda_c^{-1}\,\mathbf{I}]\,\mathbf{W} = \mathbf{0}$$

Results can only be obtained in these special cases by implementing the above simpler formulation, which also considerably increases numerical efficiency.

7 Results and discussion

The BEM formulation was implemented through a suite of C codes and applied to the buckling analysis of rectangular plates under combinations of uniform compression p_1, p_2 along x_1, x_2 directions, respectively, and edge shear p_{12} as shown in Fig 2. The critical value of a reference component of traction T_{rc} is given in terms of the critical load factor λ_c by

$$T_{rc} = \lambda_c \frac{D_3}{a^2} \tag{24}$$

where $D_3 = D_{1122} + 2\,D_{1212}$ and a the x_1-dimension of the plate as indicated in Fig. 2. For comparison purposes, the adopted material properties were the same as those used by other investigators and they are listed in Table 1.

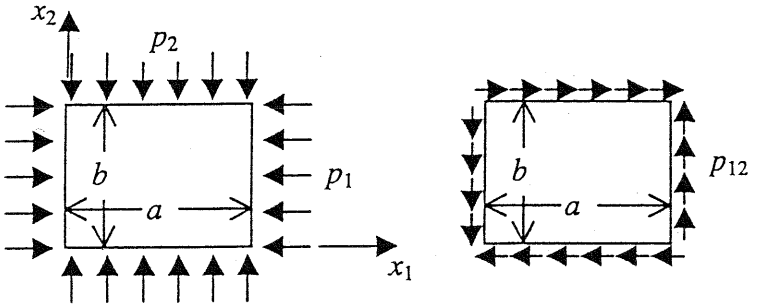

Figure 2: Geometry and loading of analysed plates

Table 1: Material properties used in solved examples

No.	Material	Plate rigidities (Nm)			
		D_{1111}	D_{2222}	D_{1212}	D_{1122}
1	Birch Plywood	11876	989.67	1000	455.25
2	Graphite/Epoxy	15151	862.18	597.5	241.41
3	Boron/Epoxy	17138.8	1542.5	510	462.749

The results for plates with various combinations of loading and boundary conditions are assembled in Tables 2 and 3. These can be compared to the corresponding published critical values obtained by other exact or approximate methods. The accuracy achieved by the BEM solution can be considered satisfactory. The predicted critical loads are consistently closer to the exact solution than those produced by the earlier BEM analysis [4].

Table 2: Critical load factor for a simply supported birch plywood square plate.

T_r	Loading	Critical load factor λ_c			
		Exact [10]	BEM [4]	BEM (present)	ANSYS
p_1	$p_1 = p_2, p_{12} = 0$	35.728	36.449	35.798	35.666
p_1	$p_2 = p_{12} = 0$	71.457	72.828	71.519	71.332
p_2	$p_1 = p_{12} = 0$	47.587	49.117	47.679	47.504
p_1	$p_2 = 2p_1, p_{12} = 0$	21.149	21.612	21.190	21.114
p_1	$p_2 = -p_1, p_{12} = 0$	63.450	65.293	63.578	
p_{12}	$p_1 = p_2 = 0$	156.359[a]	158.039	154.025	152.101
p_1	$p_1 = p_2 = p_{12}$		32.687	34.226	34.129

[a]Rayleigh-Ritz method

The performance of the developed computer code was also compared to that of a general-purpose finite element program [11] using comparable meshes, that is, a total of 40 boundary elements and 50 domain cells in BEM analyses compared to 100 8-node finite elements (Shell93, [11]). Table 2 shows that FEM

always underestimates the critical factor but otherwise its accuracy is almost the same as that of the present BEM formulation. This is sufficient evidence for accepting the present BEM results listed in Table 3 as very reliable.

Table 3. Critical load factor for clamped square graphite/epoxy plates

T_r	Loading	Critical load factor λ_c		
		BEM [4]	BEM (present)	ANSYS
p_1	$p_2 = p_{12} = 0$	481.213	466.744	456.899
p_2	$p_1 = p_{12} = 0$	168.161	160.105	156.787
p_1	$p_1 = p_2, p_{12} = 0$		142.641	138.605
p_1	$p_2 = 2p_1, p_{12} = 0$		75.519	74.090

As a further test of the accuracy and versatility of the developed model, results were also obtained for mid-plane symmetric laminates made of boron/epoxy with unidirectional reinforcement in various orientations. The rigidities of these plates are given in Table 1 for the reinforcement direction $\theta = 0°$. The results are plotted in Fig. 4 for the clamped plate case. It is worth noting that for $\theta \neq 0°$, plate rigidities D_{1112} and D_{2212} are non-zero as well. Whitney's original predictions using the Ritz method [12] as well as ANSYS results are shown on the same graph. The quality of these BEM results is consistent with that observed earlier for all values of θ.

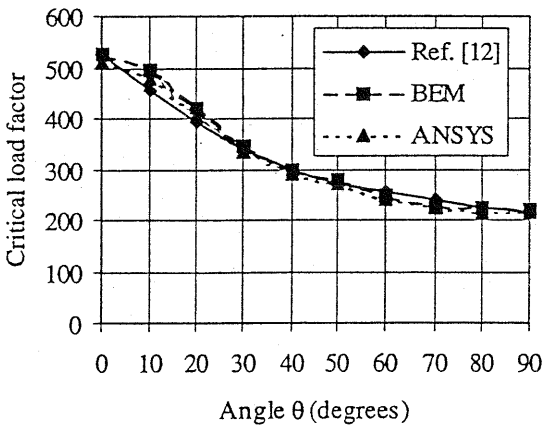

Figure 3: Critical load factor for square clamped mid-plane symmetric laminates

8 Conclusions

It has been confirmed that BEM can produce very accurate predictions of buckling load in the case of anisotropic laminate plates. The efficiency of the method should be further tested on more complex examples of non-uniform geometry, loading and support conditions. With regard to in-plane loading

producing non-uniform membrane stress distributions, some work has already been carried out towards a BEM solution for this pre-buckling equilibrium state based on a stress function formulation similar to that developed earlier for isotropic plates [6].

It is expected that the removal of domain modelling due to the presence of irreducible domain integrals would improve the efficiency of the BEM solution. A scheme based on the concept of dual reciprocity has actually been devised for isotropic plates [13] its efficiency may not however be much greater than that of the present formulation which has the additional advantage of greater flexibility in modelling plates of arbitrary shape.

Another possible extension of the proposed methodology would be the modelling of the particular type of anisotropy exhibited by laminates, known as bending-stretching coupling. This can be achieved by coupling the BEM membrane stress and buckling solutions through irreducible domain integrals which are then accounted for in the algorithm through an iterative process.

References

[1] Timoshenko, S. & Gere, J.M., *Theory of Elastic Stability*, McGraw-Hill: New York, 1961.

[2] Costa, J.A. & Brebbia, C.A., Elastic buckling of plates using the boundary element method, *Boundary Elements VII*, eds. C.A. Brebbia & G. Maier, Springer-Verlag: Berlin, pp. 4.29-4.42, 1985.

[3] Shi, G. & Bezine, G., Buckling analysis of orthotropic plates by boundary element method. *Mech. Res. Comm.*, **17(1)**, pp. 1-7, 1990.

[4] Shi, G., Flexural vibration and buckling analysis of orthotropic plates by the boundary element method, *Int. J. Solids Structures*, **26(12)**, pp. 1351-1370, 1990.

[5] Syngellakis, S. & Kang, M., A boundary element solution of the plate-buckling problem, *Eng. Anal. Bound. Elem.* **4(2)**, pp. 75-81, 1987.

[6] Syngellakis, S. & Elzein, A., Plate buckling loads by the boundary element method, *Int. J. Num. Meth. Eng.*, 37, 1994.

[7] Budiansky, B., Theory of buckling and post-buckling behavior of elastic structures, *Advances in Applied Mechanics*, Vol. 14, ed. C.S. Yih, Academic Press: New York, pp. 1-65, 1974.

[8] Shi G. & Bezine, G., A general boundary integral formulation for the anisotropic plate bending problems, *J. Comp. Mat.*, **22**, pp. 694-716, 1988.

[9] Press, W.H., Teukolsky, S.A., Vetterling, W.T. & Flannery, B.P., *Numerical Recipes in C*, Cambridge University Press: Cambridge, 1992.

[10] Lekhnitskii, S.G., *Anisotropic plates*, Gordon & Breach: New York, 1968.

[11] ANSYS 5.7, ANSYS Inc., Canonsburg, PA, 2000.

[12] Whitney, J.M., *Structural Analysis of Laminated Anisotropic Plates*, Technomic: Lancaster, Pa., 1987.

[13] Elzein A. & Syngellakis, S. Dual reciprocity in boundary element formulations of the plate buckling problem, *Eng. Anal. Bound. Elem.*, **9**, pp. 175-184, 1992.